Desalination and Water Treatment
www.deswater.com

doi: 10.1080/19443994.2014.995132

57 (2016) 4494–4501
February

Taylor & Francis
Taylor & Francis Group

Synthesis of high-performance nitrogen-containing porous carbon and adsorption properties towards metal ions

Wen-Xia Zhou[a], Tuo-Ping Hu[a,*], Jian-Feng Gao[a], Xi Chen[a], Wei-Guang Ping[a], Chin-Chuan Wei[b], Fuqiang An[b,*]

[a]*Chemical Department, North University of China, Taiyuan 030051, P.R. China, Tel. +86 351 3921414; emails: zhouwenxia@126.com (W.-X. Zhou), 2211274449@qq.com (T.-P. Hu), gaojianfeng@126.com (J.-F. Gao), 42256827@qq.com (X. Chen), huamunianhua@qq.com (W.-G. Ping)*
[b]*Biochemistry/Biophysics, Southern Illinois University, Edwardsville, IL, USA, Tel. +01 618 650 6454; email: cwei@siue.edu (C.-C. Wei), Tel. +86 351 3923197; Fax: +86 351 3922118; email: anfuqiang@nuc.edu.cn (F. An)*

Received 13 February 2014; Accepted 28 November 2014

ABSTRACT

Waste water containing metal ions is one of the main pollution sources of surface water and groundwater, and must be removed effectively. In this paper, nitrogen-containing porous carbons, the 800KH-H_2O and the 800KH-NH_3, were synthesized using sunflower plates as the major carbon source carbonized at 800°C and activated with distilled water and concentrated aqueous ammonia at the same temperature. The porous carbons were characterized by surface area analyzer, Fourier transform infrared, element analysis, and scanning electron microscopy. The adsorption properties of the porous carbons toward metal ions were studied by batch methods. The test results show that the average pore diameter of porous carbon is smaller than 2 nm, and nitrogen-containing chemical groups were formed on its surface. The adsorption capacities of the 800KH-NH_3 toward Pb^{2+} are as high as 786 mg g^{-1} due to its developed pore structure and nitrogen-containing chemical groups. The adsorption process could be well described by the intraparticle mass transfer diffusion model and the Langmuir–Freundlich model.

Keywords: Porous carbon; Adsorption; Heavy metal ion; Sunflower plate

---

1. Introduction

Industrial development has greatly polluted surface water and groundwater resulting from heavy metal ions. Heavy metal ions possess high toxic effect to animals, plants, and human beings. Unlike organic contaminants, heavy metal ions were not biodegradable and tend to accumulate in living organisms and many of them were known to be toxic or carcinogenic even at very low concentration. Therefore, the effective removal of heavy metal ions from water is very necessary and has attracted considerable research and practical interest. Adsorption method, as an effective and economical method, was used widely to remove heavy metal ions from aqueous solutions. Various materials, including modified and unmodified inorganic adsorbents [1–24], metal oxides [25–29], and chelating resin [30–38], have been reported to remove heavy metal ions from aqueous solutions. However, most of these adsorbents suffer from low adsorption capacities or

---

*Corresponding authors.

hard preparation procedures. Therefore, it is necessary to seek more effective adsorbents to remove metal ions from aqueous solutions.

Porous carbons possess developed pore structure, high specific surface, and are easy to surface modification. This makes it widely used as adsorbent [14–24], catalyst supports [39–42], etc. Biomass and polymers are the commonly used precursors to prepare porous carbons [14–18,20–24]. In general, porous carbon was prepared at higher temperature and has few surface functional groups on its surface [20–24]. So, the adsorption of porous carbon mainly uses its physical adsorption mechanism, and the adsorption capacity is poor. In order to improve its adsorption property, surface chemical modification of porous carbon is desired and many methods have been developed. For example, nitrogen-containing chemical groups are introduced to the porous carbon after treatment with NH_3 or HNO_3 [42–44]. This chemical modification improves the adsorption properties markedly.

In this work, nitrogen-containing porous carbons of high surface area and large pore volume were synthesized using sunflower plates as the major carbon source carbonized at 800℃ and activated with distilled water and concentrated aqueous ammonia at 800℃, respectively. The pore structure was determined, and the surface chemical groups of resultant porous carbon were characterized. Its adsorption properties for heavy metal ions were investigated.

2. Experiments

2.1. Synthesis of porous carbon

At first, sunflower plate was washed and dried at 100℃ for 24 h. It was then pulverized and sieved. A certain amount of sunflower plate powder (100–125 μm) was carbonized in charcoal furnace at 800℃ for 2 h with heating rate of 3℃ min^{-1} and N_2 flow of 50 ml min^{-1}, and then activated with distilled water and concentrated aqueous ammonia at 800℃, respectively. Finally, the resultant samples were washed with distilled water until neutral and then, dried at 80℃ for 24 h. The unactivated porous carbon, the activated porous carbon treated with distilled water and concentrated aqueous ammonia were denoted as 800KH, 800KH-H_2O, and 800KH-NH_3, respectively.

2.2. Characterizations

The surface area properties were measured with JWGB JW-BK132F surface area analyzer (Beijing, China). The surface area was calculated by the Brunauer–Emmett–Teller (BET) method. The pore size distribution (PSD) was calculated by a Barret-Joyner-Halenda (BJH) method using nitrogen adsorption data. The micropore volume was obtained from Horvaih-Kawazoe (HK) method, and the total pore volume (V_{Tot}) was estimated from the adsorbed amount at a relative pressure P/P_0 of 0.995. Scanning electron microscopy images were obtained using S-4800 field emission microscope (Hitachi, Japan). Fourier transform infrared (FT-IR) spectrum of the sample was measured on a FTIR4800S spectrometer using the usual KBr pellet technique (Shimadzu, Japan). The element content was measured with Vario EL elemental analyzer (Elementar, Germany).

2.3. Adsorption experiments

About 0.01 g of porous carbon and 25 ml aqueous solution of heavy metal ion of different initial concentrations at pH of 4 were directly introduced into several conical flasks. These conical flasks were shaken in a shaker at 20℃. After reaching the adsorption equilibrium (12 h), the equilibrium concentration (C_e) of the heavy metal ion solution was determined using Prodigy ICP-ACE (Leeman Lab, America). Equilibrium adsorption capacity (Q_e) was calculated according to the following equation (Eq. (1)).

$$Q_e = [(C_0 - C_e)/m] \times V \tag{1}$$

where C_0 and C_e are the initial and equilibrium concentrations of the heavy metal ions in the solution (mg L^{-1}), V is the volume of the solution (L), and m is the dosage of the adsorbent (g).

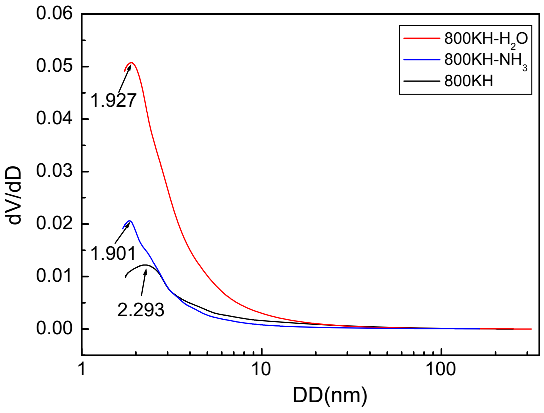

Fig. 1. PSD of porous carbons.

Table 1
The pore structure parameters

Samples	S_{BET} ($m^2 g^{-1}$)	V_{total} ($cm^3 g^{-1}$)	$V_{micropore}$ ($cm^3 g^{-1}$)	$V_{mesopore}$ ($cm^3 g^{-1}$)	Pore size (nm)
800KH	221.09	0.147	0.075	0.072	2.293
800KH-H_2O	370.61	0.244	0.146	0.098	1.927
800KH-NH_3	311.79	0.259	0.168	0.091	1.901

3. Result and discussion

3.1. Characterization of porous carbon structure

The PSD and most average pore diameter of samples were shown in Fig. 1. The pore properties of the 800KH, 800KH-H_2O, and 800KH-NH_3 are listed in Table 1.

The average pore diameter of 800KH-H_2O and 800KH-NH_3 of around 1.9 nm indicates that the porous carbon is microporous. It can be seen that the BET special surface area and pore volume increase but average pore diameter decreases after activation with distilled water and concentrated aqueous ammonia. The decrease in pore size was due to the modification of the internal surface by activation. The increase in BET special surface area and pore volume indicate that the number of pore increases.

The SEM images of samples before and after the H_2O or NH_3 activation are shown in Fig. 2.

The surface of the 800KH is relatively coarse as some carbon particles fill the big pore and are attached to the surrounding surface. When the 800KH is activated, the surface becomes smooth. This is because the filled and attached carbon particles are removed. So, the BET special surface area and pore volume increases. This is consistent with the former structure analysis.

The presence of the nitrogen-containing groups in the prepared porous carbons was confirmed by FT-IR spectroscopy (Fig. 3) and elemental analysis (Table 2).

In the spectra of the 800KH-H_2O and 800KH-NH_3, an intense band appeared at 710/711 cm^{-1}, and the intensity of the 800KH-NH_3 is higher than that of the 800KH-H_2O. These bands are assigned to the characteristic absorption of the N–H bond. The peak at 1,556 cm^{-1} in the spectrum of the 800KH-H_2O is assigned to the characteristic absorption of the -NO_2 group. Together with the elemental analysis results, the O content of the 800KH-H_2O is higher than that of the 800KH-NH_3 the N in the 800KH-NH_3 mainly exists in the form of amino group, while it exists in the form of nitro group in the 800KH-H_2O. This also can be evidenced from the adsorption experiment.

Additionally, it can also be seen from the elemental analysis that the N and C content of the porous carbon increases slightly after activation with distilled water and concentrated aqueous ammonia. The reason may be that the composition and structure of the porous carbon materials are changed in the activation procedure. These can be evidenced from the data of Table 1.

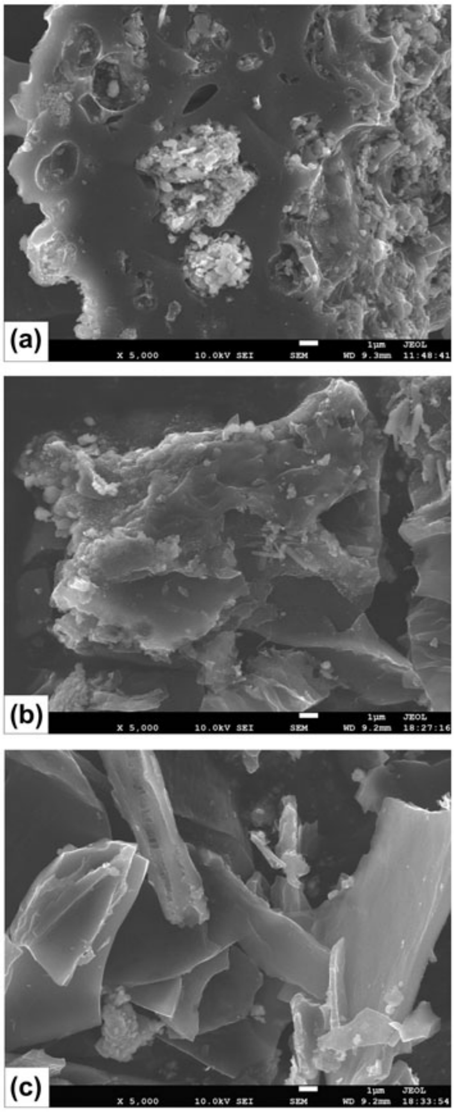

Fig. 2. SEM images of porous carbons: (a) 800KH, (b) 800KH-H_2O, and (c) 800KH-NH_3.

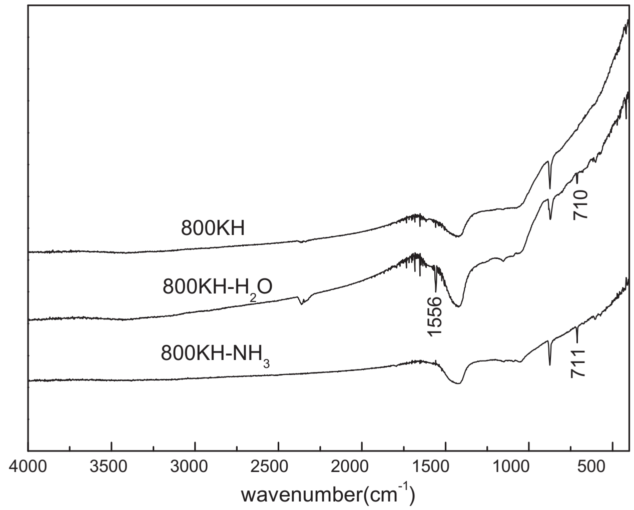

Fig. 3. FT-IR spectra.

3.2. *Adsorption properties of porous carbon toward metal ions*

The kinetic adsorption curve of the 800KH, 800KH-H_2O, and 800KH-NH_3 toward metal ions was shown in Fig. 4.

The saturated adsorption capacity of the 800KH, 800KH-H_2O, and the 800KH-NH_3 toward Pb^{2+} are 340, 514, and 786 mg g^{-1}, respectively. For all the metal ions studied (kinetic adsorption curves of 800KH and 800KH-H_2O toward Cd^{2+}, Cu^{2+}, and Zn^{2+} were omitted), the adsorption capacity of the 800KH-H_2O and 800KH-NH_3 is higher than that of 800KH. This is attributed to the developed pore structure, the high specific surface, and the surface modification with the functional groups in the 800KH-H_2O and 800KH-NH_3 structures. Therefore, the adsorption capacity is enhanced after activation. Moreover, the adsorption capacity of the 800KH-H_2O is lower than that of 800KH-NH_3 although the specific surface area of the former is higher than that of the latter. The reason may be that the 800KH-NH_3 possesses more amino groups on its internal surface than the 800KH-H_2O, which can be evidenced with the FT-IR spectra and elemental analysis.

Table 2
Elemental analysis results

Samples	Weight (g)	N (%)	C (%)	H (%)	O (%)	S (%)
800KH	2.5970	1.42	59.79	2.717	17.312	0.205
800KH-NH_3	2.2990	1.72	63.03	0.805	10.263	0.282
800KH-H_2O	2.2530	2.09	66.32	1.576	11.404	0.210

Importantly, the 800KH, the 800KH-H_2O, and the 800KH-NH_3 prepared in this study possess higher adsorption capacity toward metal ions than previously reported porous carbons. The comparisons are shown in Table 3. This demonstrates that the 800KH-NH_3 possesses very strong adsorption ability and high affinity for metal ions, and it can be used to remove effectively metal ions.

Kinetic parameters can give important information for the efficiency of adsorption. To analyze the adsorption rate of the Pb^{2+} on 800KH-NH_3, three kinetic models including the Lagergren-first-order model, pseudo-second-order kinetic model, and intraparticle mass transfer diffusion model were used to analyze the dynamics of the adsorption process.

The Lagergren-first-order model is expressed as Eq. (2):

$$\ln(Q_e - Q_t) = \ln Q_e - kt \tag{2}$$

where Q_t (mg g^{-1}) is the adsorption amount at time t (h); Q_e (mg g^{-1}) is the equilibrium adsorption amount; and k_1 (h^{-1}) is the adsorption rate constant. k_1 can be determined experimentally by plotting of ln ($Q_e - Q_t$) vs. t.

The pseudo-second-order kinetic model is expressed as Eq. (3):

$$\frac{t}{Q_t} = \frac{1}{k_2 Q_e^2} + \frac{t}{Q_e} \tag{3}$$

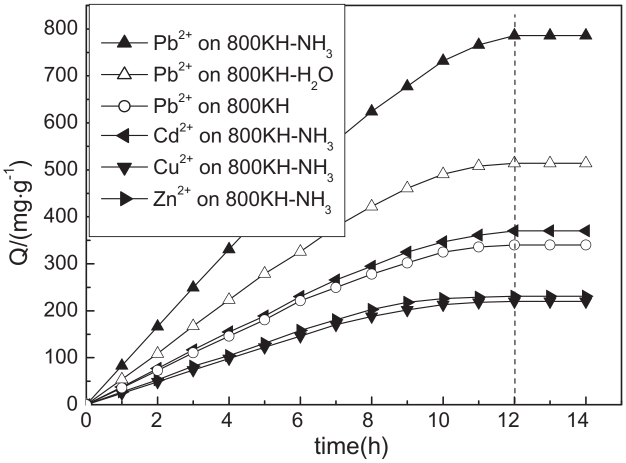

Fig. 4. Adsorption kinetic curves of 800KH, 800KH-H_2O, and 800KH-NH_3 for metal ions temperature: 20℃; pH 4.

Table 3
Comparisons of adsorption capacity (mg/g) of 800KH-NH_3 by other AC adsorbents

	Metal ion				
Precursors of AC adsorbents	Pb^{2+}	Cd^{2+}	Cu^{2+}	Zn^{2+}	References
Sunflower plates	786	370	220	231	This study
Hemp fiber	47	–	–	–	[14]
Lapsi seed	147	–	–	39.9 (Ni^{2+})	[16]
Plum kernels	7.2	–	–	–	[17]
Jacaranda fruit	5	–	–	–	[17]
Ficus carica	–	–	18	12 (Ni^{2+})	[18]
Carboxylic functionalized activated carbon	80	27.5	–	–	[19]
Apple pulp	11	–	–	8	[20]
Maso and Ma bamboo	1.90	0.67	1.91	0.66 (Cr^{3+})	[21]
Cyclohexanol	101.05	75.84	50.37	–	[22]
Coconut button	44.4	40.8 (Hg^{2+})	36.4	–	[23]
Melocanna baccifera	–	0.1 (Ni^{2+})	–	0.1	[24]

Table 4
Kinetic parameters of Pb^{2+} on 800KH-NH_3

Lagergren-first-order			Pseudo-second-order			Intra-particle diffusion		
Q_e	k_1	R^2	Q_e	k_2	R^2	k_{id}	c	R^2
1,460.7	0.3178	0.8924	5,000	3.5×10^{-6}	0.8114	308.1	−261.3	0.9937

where k_2 is the rate constant of the pseudo-second-order adsorption ($\mathrm{g\,mg^{-1}\,h^{-1}}$). k_2 can be determined from plotting (t/Q_t) vs. t.

The intraparticle mass transfer diffusion model is expressed as Eq. (4):

$$Q_t = k_{id} t^{1/2} + c \tag{4}$$

where c is the intercept ($\mathrm{mg\,g^{-1}}$) and k_{id} is the intraparticle diffusion rate constant ($\mathrm{mg\,g^{-1}\,min^{1/2}}$), which can be evaluated from the slope of the linear plot of Q_t vs. $t^{1/2}$.

The kinetic parameters and correlation coefficients (R^2) are summarized in Table 4. Compared with the Lagergren-first-order model and pseudo-second-order kinetic model, the correlation coefficient (R^2) of the intraparticle mass transfer diffusion model is closer to 1.0. This shows that the intraparticle mass transfer diffusion model is more suitable to describe the adsorption process of Pb^{2+} on 800KH-NH_3.

In order to research the adsorption behavior of Pb^{2+} ions on 800KH-NH_3, it is important to have a satisfactory description of the quantitative relationship between the two phases in the adsorption system. The adsorption isotherms of 800KH, 800KH-H_2O, and 800KH-NH_3 for Pb^{2+} ion were thus determined and are shown in Fig. 5. The adsorption isotherms were attempted to be fitted with the Langmuir (Eq. 5), Freundlich (Eq. 6), Sips (Eq. 7), Temkin (Eq. 8), and Dubunin–Radushkevich (D–R) model (Eq. 9), respectively [45–47].

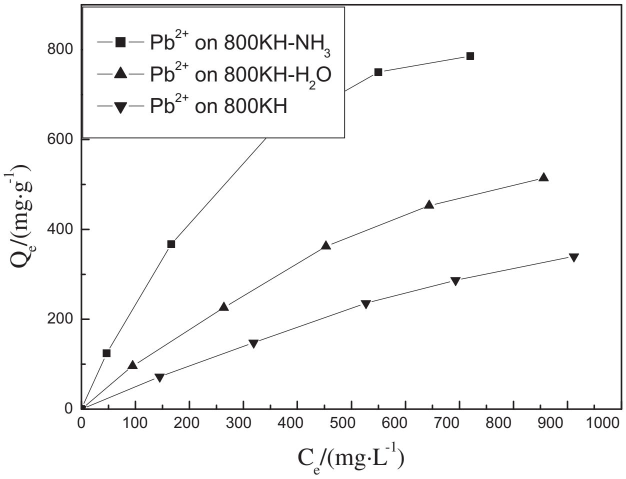

Fig. 5. Adsorption isotherms of 800KH-NH_3 towards Pb^{2+} temperature: 20℃; time: 12 h; pH.

Table 5
Parameters for plotting adsorption isotherms Pb^{2+}

Model	Langmuir		Freundlich		Sips		Temkin		D–R	
Parameter	K	Q_0	n	k	b	m	B_T	b_T	Q_0	K_{ad}
	0.0025	1,250	1.51	11.16	0.0095	4.02	243.93	9.99	609.96	0.0006

Table 6
Adsorption linear regression equations of 800KH-NH_3 towards Pb^{2+}

Adsorption model	Linear regression equation	R^2
Langmuir	$C_e/Q_e = 0.0008C_e + 0.3241$	0.9971
Freundlich	$\ln Q_e = 0.661 \ln C_e + 2.4119$	0.9921
Sips isotherm	$Q_e = 858.8 \times 0.0095 \times {C_e}^{4.02}/(1 + 0.0095 \times {C_e}^{4.02})$	0.9991
Temkin	$Q_e = 243.93 \ln C_e - 837.94$	0.9786
Dubinin–Radushkevich	$\ln Q_e = -0.0006\varepsilon^2 + 6.4134$	0.8631

$$C_e/Q_e = C_e/Q_0 + 1/(KQ_0) \tag{5}$$

$$\ln Q_e = \ln k + (1/n)\ln C_e \tag{6}$$

$$Q_e = Q_0 b {C_e}^m/(1 + b{C_e}^m) \tag{7}$$

$$Q_e = B_T \ln C_e + B \ln A_T \tag{8}$$

$$\ln Q_e = \ln Q_0 - K_{ad}\varepsilon^2 \tag{9}$$

where C_e (mg L^{-1}) is the equilibrium concentration, Q_e (mg g^{-1}) is the equilibrium adsorption capacity, Q_0 (mg g^{-1}) is the monolayer sorption capacity, K (L mg^{-1}) is the Langmuir constant related to the adsorption energy, k is adsorption equilibrium constant which represents the strength of the adsorptive bond, n is the heterogeneity factor which represents the bond distribution, b is the adsorption equilibrium constant, and m the dissociation parameter, $B_T = (RT)/b_T$, b_T is related to the heat of adsorption, A_T (L min^{-1}) is the equilibrium adsorption constant corresponding to the maximum adsorption energy, K_{ad} (mol^2 kJ^{-2}) is a constant related to the adsorption energy, ε (J mol^{-1}) was the Polanyi potential, $\varepsilon = RT \ln(1 + 1/C_e)$. In Sips isotherm, if the value of b approaches 0, the Sips isotherm will become a Freundlich isotherm. While the value of m equals 1 or is closer to 1, the Sips isotherm equation reduces to the Langmuir equation; that is, adsorption takes place on homogeneous surface.

The fitting parameters of the adsorption data to the equations are listed in Table 5 and the linear regression equations and the correlation coefficient are described in Table 6.

From the R^2 summarized in Table 6, it can be concluded that the Langmuir and Freundlich equations fit best to the experimental data ($R^2 > 0.99$). The value of b (0.0095) in Sips isotherm approaches 0, and this indicates that the Freundlich model is more appropriate to describe the adsorption behavior than the Langmuir model. Thus, the applicability of monolayer coverage of metal ions on the surface of the activated carbon is confirmed.

4. Conclusion

High-performance nitrogen-containing porous carbons were synthesized successfully from the sunflower plates carbonized at 800℃ and activated with distilled water and concentrated aqueous ammonia at the same temperature. The 800KH-H_2O and the 800KH-NH_3 porous carbons were produced. The BET special surface areas are as high as 370.61 and 311.79 m^2 g^{-1}, respectively. The pore size is also less than 2 nm. These nitrogen-containing porous carbons display high adsorption capacities for heavy metal ions due to its developed pore structure and nitrogen-containing functional groups. The adsorption capacity of the 800KH-NH_3 toward Pb^{2+} was as high as 786 mg g^{-1}. The adsorption process could be well described by the intraparticle mass transfer diffusion model and Langmuir–Freundlich model.

Acknowledgments

The authors gratefully acknowledge the financial support of this work by the International Science & Technology Cooperation Program of China (No. 2011DFA51980), Shanxi Science & Technology Cooperation Program of China (No. 2011DFA51980), and Science Foundation of Shanxi Province (No. 20130321022-02, 2013021012-3).

Funding

The authors gratefully acknowledge the financial support of this work by the International Science & Technology Cooperation Program of China [Grant Number (No. 2011DFA51980)]; Shanxi Science & Technology Cooperation Program of China [Grant Number (No. 2011DFA51980)]; Science Foundation of Shanxi Province [Grant Numbers (No. 20130321022–02, 2013021012–3)].

References

[1] X.Y. Zhao, Y.J. Zhu, J. Zhao, B.Q. Lu, F. Chen, C. Qi, J. Wu, Hydroxyapatite nanosheet-assembled microspheres: Hemoglobin-templated synthesis and adsorption for heavy metal ions, J. Colloid Interface Sci. 416 (2014) 11–18.

[2] M.H. Wang, R.J. Qu, C.M. Sun, P. Yin, H. Chen, Dynamic adsorption behavior and mechanism of transition metal ions on silica gels functionalized with hydroxyl- or amino-terminated polyamines, Chem. Eng. J. 221 (2013) 264–274.

[3] D. Božić, M. Gorgievski, V. Stanković, N. Štrbac, S. Šerbula, N. Petrović, Adsorption of heavy metal ions by beech sawdust-kinetics, mechanism and equilibrium of the process, Ecol. Eng. 58 (2013) 202–206.

[4] X.S. Li, S.L. Liu, Z.Y. Na, D.N. Lu, Z. Liu, Adsorption, concentration, and recovery of aqueous heavy metal ions with the root powder of *Eichhornia crassipes*, Ecol. Eng. 60 (2013) 160–166.

[5] M. Najafi, Y. Yousefi, A.A. Rafati, Synthesis, characterization and adsorption studies of several heavy metal ions on amino-functionalized silica nano hollow sphere and silica gel, Sep. Purif. Technol. 85 (2012) 193–205.

[6] T.S. Anirudhan, S. Jalajamony, S.S. Sreekumari, Adsorption of heavy metal ions from aqueous solutions by amine and carboxylate functionalised bentonites, Appl. Clay Sci. 65–66 (2012) 67–71.

[7] Claudiane Ouellet-Plamondon, Rod J. Lynch, Abir Al-Tabbaa, Comparison between granular pillared, organo- and inorgano-organo-bentonites for hydrocarbon and metal ion adsorption, Appl. Clay Sci. 67–68 (2012) 91–98.

[8] S.S. Gupta, K.G. Bhattacharyya, Kinetics of adsorption of metal ions on inorganic materials: A review, Adv. Colloid Interface Sci. 162 (2011) 39–58.

[9] Q.H. Wang, X.J. Chang, D.D. Li, Z. Hu, R.J. Li, Q. He, Adsorption of chromium(III), mercury(II) and lead(II) ions onto 4-aminoantipyrine immobilized bentonite, J. Hazard. Mater. 186 (2011) 1076–1081.

[10] A.D. Papandreou, C.J. Stournaras, D. Panias, I. Paspaliaris, Adsorption of Pb(II), Zn(II) and Cr(III) on coal fly ash porous pellets, Miner. Eng. 24 (2011) 1495–1501.

[11] Y.F. Tao, Y. Qiu, S.Y. Fang, Z.Y. Liu, Y. Wang, J.H. Zhu, Trapping the lead ion in multi-components aqueous solution by natural clinoptilolite, J. Hazard. Mater. 180 (2010) 282–288.

[12] M.Q. Jiang, X.Y. Jin, X.Q. Lu, Z.L. Chen, Adsorption of Pb(II), Cd(II), Ni(II) and Cu(II) onto natural kaolinite clay, Desalination 252 (2010) 33–39.

[13] Q.Z. Li, L.Y. Chai, Q.W. Wang, Z.H. Yang, H.X. Yan, Y.Y. Wang, Fast esterification of spent grain for enhanced heavy metal ions adsorption, Bioresour. Technol. 101 (2010) 3796–3799.

[14] M. Vukčević, B. Pejić, A. Kalijadis, I. Pajić-Lijaković, M. Kostić, Z. Laušević, M. Lauševic, Carbon materials from waste short hemp fibers as a sorbent for heavy metal ions-mathematical modeling of sorbent structure and ions transport, Chem. Eng. J. 235 (2014) 284–292.

[15] M. Kılıç, Ç. Kırbıyık, Ö. Çepelioğullar, A.E. Pütün, Adsorption of heavy metal ions from aqueous solutions by bio-char, a by-product of pyrolysis, Appl. Surf. Sci. 283 (2013) 856–862.

[16] R.M. Shrestha, I. Varga, J. Bajtai, M. Varga, Design of surface functionalization of waste material originated charcoals by an optimized chemical carbonization for the purpose of heavy metal removal from industrial waste waters, Microchem. J. 108 (2013) 224–232.

[17] H. Treviño-Cordero, L.G. Juárez-Aguilar, D.I. Mendoza-Castillo, V. Hernández-Montoya, A. Bonilla-Petriciolet, M.A. Montes-Morán, Synthesis and adsorption properties of activated carbons from biomass of Prunus domestica and Jacaranda mimosifolia for the removal of heavy metals and dyes from water, Ind. Crops Prod. 42 (2013) 315–323.

[18] V.K. Gupta, D. Pathania, S. Sharma, Adsorptive remediation of Cu(II) and Ni(II) by microwave assisted H_3PO_4 activated carbon, Arab. J. Chem. (2013, in press), http://dx.doi.org/10.1016/j.arabjc.2013.11.006

[19] M. Machida, B. Fotoohi, Y. Amamo, L. Mercier, Cadmium(II) and lead(II) adsorption onto hetero-atom functional mesoporous silica and activated carbon, Appl. Surf. Sci. 258 (2012) 7389–7394.

[20] T. Depci, A.R. Kulb, Y. Őnal, Competitive adsorption of lead and zinc from aqueous solution on activated carbon prepared from Van apple pulp: Study in single- and multi-solute systems, Chem. Eng. J. 200–202 (2012) 224–236.

[21] S.F. Lo, S.Y. Wang, M.J. Tsai, L.D. Lin, Adsorption capacity and removal efficiency of heavy metal ions by Moso and Ma bamboo activated carbons, Chem. Eng. Res. Des. 90 (2012) 1397–1406.

[22] M.A. Tofighy, T. Mohammadi, Adsorption of divalent heavy metal ions from water using carbon nanotube sheets, J. Hazard. Mater. 185 (2011) 140–147.

[23] T.S. Anirudhan, S.S. Sreekumari, Adsorptive removal of heavy metal ions from industrial effluents using activated carbon derived from waste coconut buttons, J. Environ. Sci. 23 (2011) 1989–1998.

[24] H. Lalhruaitluanga, M.N.V. Prasad, K. Radha, Potential of chemically activated and raw charcoals of Melocanna baccifera for removal of Ni(II) and Zn(II) from aqueous solutions, Desalination 271 (2011) 301–308.

[25] K.Y. Kumar, H.B. Muralidhara, Y.A. Nayaka, J. Balasubramanyam, H. Hanumanthappa, Low-cost synthesis of metal oxide nanoparticles and their application in adsorption of commercial dye and heavy metal ion in aqueous solution, Powder Technol. 246 (2013) 125–136.

[26] Y.Z. Xiao, H.F. Liang, W. Chen, Z.C. Wang, Synthesis and adsorption behavior of chitosan-coated $MnFe_2O_4$ nanoparticles for trace heavy metal ions removal, Appl. Surf. Sci. 285P (2013) 498–504.

[27] A.A. Farghali, M. Bahgat, A. Enaiet Allah, M.H. Khedr, Adsorption of Pb(II) ions from aqueous solutions using copper oxide nanostructures, Beni-Suef Univer. J. Basic Appl. Sci. 2 (2013) 61–71.

[28] P. Tao, M.H. Shao, C.W. Song, S.H. Wu, M.R. Cheng, Z. Cui, Preparation of porous and hollow Mn_2O_3 microspheres and their adsorption studies on heavy metal ions from aqueous solutions, J. Ind. Eng. Chem. 20 (2013) 3128–3133.

[29] J. Song, H. Kong, J. Jang, Adsorption of heavy metal ions from aqueous solution by polyrhodanine-encapsulated magnetic nanoparticles, J. Colloid Interface Sci. 359 (2011) 505–511.

[30] C. Cheng, J.N. Wang, X. Yang, A.M. Li, C. Philippe, Adsorption of Ni(II) and Cd(II) from water by novel chelating sponge and the effect of alkali-earth metal ions on the adsorption, J. Hazard. Mater. 264 (2014) 332–341.

[31] T.M. Mututuvari, C.D. Tran, Synergistic adsorption of heavy metal ions and organic pollutants by supramolecular polysaccharide composite materials from cellulose, chitosan and crown ether, J. Hazard. Mater. 264 (2014) 449–459.

[32] L.F. Koong, K.F. Lam, J. Barford, G. McKay, A comparative study on selective adsorption of metal ions using animated adsorbents, J. Colloid Interface Sci. 395 (2013) 230–240.

[33] T. Oshima, S. Ishizaka, H. Morizono, K. Ohe, Y. Baba, Adsorption behavior of metal ions on alkylhistidine extractant impregnated resins: Effect of functional groups of histidine, Sep. Purif. Technol. 114 (2013) 11–16.

[34] F. Ji, C.L. Li, B. Tang, J.H. Xu, G. Lu, P. Liu, Preparation of cellulose acetate/zeolite composite fiber and its adsorption behavior for heavy metal ions in aqueous solution, Chem. Eng. J. 209 (2012) 325–333.

[35] M.H. Min, L.D. Shen, G.S. Hong, M.F. Zhu, Y. Zhang, X.F. Wang, Y.M. Chen, B.S. Hsiao, Micro-nano structure poly(ether sulfones)/poly(ethyleneimine) nanofibrous affinity membranes for adsorption of anionic dyes and heavy metal ions in aqueous solution, Chem. Eng. J. 197 (2012) 88–100.

[36] M. Addy, B. Losey, R. Mohseni, E. Zlotnikov, A. Vasiliev, Adsorption of heavy metal ions on mesoporous silica-modified montmorillonite containing a grafted chelate ligand, Appl. Clay Sci. 59–60 (2012) 115–120.

[37] L.J. Li, F.Q. Liu, X.S. Jing, P.P. Ling, A.M. Li, Displacement mechanism of binary competitive adsorption for aqueous divalent metal ions onto a novel IDA-chelating resin: Isotherm and kinetic modeling, Water Res. 45 (2011) 1177–1188.

[38] F.Q. An, B.J. Gao, X. Dai, M. Wang, X.H. Wang, Efficient removal of heavy metal ions from aqueous solution using salicylic acid type chelate adsorbent, J. Hazard. Mater. 192 (2011) 956–962.

[39] L. Jiang, H. Fu, L. Wang, G. Mu, B. Jiang, W. Zhou, R. Wang, Tungsten carbide/porous carbon composite as superior support for platinum catalyst toward methanol electro-oxidation, Mater. Res. Bull. 49 (2014) 480–486.

[40] Y.J. Hsueh, C.C. Yu, K.R. Lee, C.J. Tseng, B.J. Su, S.K. Wu, L.C. Weng, Ordered porous carbon as the catalyst support for proton-exchange membrane fuel cells, Int. J. Hydrogen Energy 38 (2013) 10998–11003.

[41] A.Y. Lo, C.T. Hung, N. Yu, C.T. Kuo, S.B. Liu, Syntheses of carbon porous materials with varied pore sizes and their performances as catalyst supports during methanol oxidation reaction, Appl. Energy 100 (2012) 66–74.

[42] Y.S. Yun, D. Kim, H.H. Park, Y. Tak, H.J. Jin, 3D hierarchical porous carbons containing numerous nitrogen atoms as catalyst supports for PEMFCs, Synth. Met. 162 (2012) 2337–2341.

[43] R. Pietrzak, XPS study and physico-chemical properties of nitrogen-enriched microporous activated carbon from high volatile bituminous coal, Fuel 88 (2009) 1871–1877.

[44] M.H. Kasnejad, A. Esfandiari, T. Kaghazchi, N. Asasian, Effect of pre-oxidation for introduction of nitrogen containing functional groups into the structure of activated carbons and its influence on Cu(II) adsorption, J. Taiwan Inst. Chem. E. 43 (2012) 736–740.

[45] C.X. Zhang, Q.Q. Qiao, J.D.A. Piper, B.C. Huang, Assessment of heavy metal pollution from a Fe-smelting plant in urban river sediments using environmental magnetic and geochemical methods, Environ. Pollut. 159 (2011) 3057–3070.

[46] S. Hena, Removal of chromium hexavalent ion from aqueous solutions using biopolymer chitosan coated with poly 3-methyl thiophene polymer, J. Hazard. Mater. 181 (2010) 474–479.

[47] R. Sips, On the structure of a catalyst surface, J. Chem. Phys. 16 (1948) 490–495.